Evidence for directed percolation universality at the onset of spatiotemporal intermittency in coupled circle maps

T.M. Janaki[a,1], Sudeshna Sinha[a,2] and Neelima Gupte[b,3]

[a]*Institute of Mathematical Sciences, Taramani, Chennai 600 113, India*[1,2]

[b] *Department of Physics, IIT Madras, Chennai 600036, India*[3]

Abstract

We consider a lattice of coupled circle maps, a model arising naturally in descriptions of solid state phenomena such as Josephson junction arrays. We find that the onset of spatiotemporal intermittency (STI) in this system is analogous to directed percolation (DP), with the transition being to an unique absorbing state for low nonlinearities, and to weakly chaotic absorbing states for high nonlinearities. We find that the complete set of static exponents and spreading exponents at all critical points match those of DP very convincingly. Further, hyperscaling relations are fulfilled, leading to independent controls and consistency checks of the values of all the critical exponents. These results lend strong support to the conjecture that the onset of STI in deterministic models belongs to the DP universality class.

[1]janaki@imsc.ernet.in

[2]sudeshna@imsc.ernet.in

[3]gupte@chaos.iitm.ernet.in

1 Introduction

Spatiotemporal intermittency (STI) in coupled map lattices (CML) has been extensively studied in varied contexts, especially as it is the precursor of fully developed spatiotemporal chaos in extended dynamical systems [1]. There are two types of motion seen in systems exhibiting STI: laminar and turbulent. The laminar region is characterized by periodic or even weakly chaotic dynamics, while no spatiotemporally regular structure can be seen in the turbulent regime. A laminar or 'inactive' site becomes turbulent or 'active' at a particular time only if at least one of its neighbours was turbulent at an earlier time, i.e., there is no spontaneous creation of turbulent sites. Hence a turbulent site can either relax spontaneously to its laminar state or contaminate its neighbours [2]. This feature is analogous to directed percolation (DP). Also, once all the sites relax spontaneously to its laminar state, the system gets trapped in this state for all time. Hence, the laminar state is "absorbing" in STI. The existence of the absorbing states led to the conjecture by Pomeau that STI in deterministic models also belongs to the DP universality class [3]. To be more precise, if the propagation rate of turbulence is below a certain threshold, the turbulent states die out and the system remains in the laminar state for all time (laminar phase/inactive phase). On the other hand, on exceeding this threshold, the turbulent states start "percolating" in spacetime (turbulent/inactive phase).

While there is substantial evidence of DP universality in stochastic models exhibiting a continuous transition to an absorbing state [4, 5], it is of considerable interest to examine the robustness of DP critical behaviour in

systems with *completely deterministic evolution rules*. To this end, Chate and Manneville introduced a simple CML [6] exhibiting STI and possessing infinitely many absorbing states. Surprisingly, it was found that not only were the exponents governing the onset of STI different from those of DP, they were also non-universal in nature [6]. This non-universal behaviour was considered to be due to the existence of travelling solitary excitations (solitons) with long life times in this model. It was argued that the existence of these solitons, which spoiled the DP nature of the universality class, was an artefact of the synchronous updating rule and asynchronous updates were tried with this model. This asynchronous update destroyed the solitons and then the static exponents were found to be consistent with DP [7]. Later it was also observed that even finite lifetime solitons could completely change the nature of transition in a weak soliton region [8]. This indicates that it is *non-trivial to map deterministic dynamics to stochastic behaviour* as various spatiotemporal structures (such as these solitons) may introduce long range correlations thereby ruining the analogy. Hence it is of considerable interest to find CMLs with regimes where there are no additional special spatiotemporal structures, which can be used as clean testbeds for checking the validity of the DP universality class.

Since the state variables of CMLs can often be identified with physical quantities (such as voltages, currents, pressures, temperatures, concentrations or velocities) in fairly realistic situations, it is conceivable that such models may suggest various experimental possibilities for observing DP, which still remains an outstanding problem [4]. Further STI is a common phenomena of many extended systems, and is seen for instance in experi-

ments on convection [9] and in the "printers instability" [10]. So if the onset of STI does in fact exhibit DP universality, then it could lead to promising candidates for observing DP in real phenomena. And indeed a recent experiment by Rupp *et al* [11] finds agreement with DP exponents at the transition to STI in a 1-dimensional system of ferrofluid spikes driven by an external oscillating magnetic field.

Now, in the last decade only the Chate-Manneville CML and its variants [8] have been studied in this context. Numerical evidence from more varied sources is required, especially in the absence of analytical results, in order to settle the question of DP universality in transitions occuring in deterministic systems. Thus, it is of considerable interest to be able to find examples of this correspondence in systems quite distinct from the Chate-Manneville class, and with qualitatively different absorbing states, that would lend credence to the Pomeau conjecture. This work provides one such example.

In this paper, we consider the coupled circle map lattice [12] which has been used to model mode-locking behaviour of the type seen in coupled oscillator systems and in diverse experimental systems such as Charge Density Waves and Josephson-Junction arrays [13]. We find that this system has regimes which show spatio-temporal intermittency, with both unique and weakly chaotic laminar regions, at different values of the nonlinearity parameter. Importantly, the solitons which spoilt the DP behaviour in the earlier studies are completely absent here. Thus we have at hand a CML without any potentially problematic coherent spatiotemporal structures, showing the onset of spatiotemporal intermittency very cleanly. This CML can then serve as a good testbed for checking the validity of the DP universality class for

4

both unique and fluctuating absorbing states.

We will now present results from this system strongly indicating that the complete set of static exponents characterising the transition to STI are completely consistent with DP, both for unique and weakly chaotic absorbing states. We will also show that the spreading exponents (dynamic exponents) for unique as well as fluctuating absorbing states agree within 3 % of those obtained in DP. Further we will demonstrate that the hyperscaling relations in case of the static as well as the spreading exponents are also satisfied. Thus we will provide two distinct examples of clean DP universality in transitions to STI, one of which constitutes the *first known example of this correspondence in a CML with an unique absorbing state*, and the other constitutes the *first example of this correspondence when there exists weakly chaotic absorbing state*.

2 Static (Bulk) Exponents

First, recall the coupled circle map lattice[14]:

$$\theta_{i,t+1} = (1-\epsilon)\,f(\theta_i,t) + \frac{\epsilon}{2}\,(f(\theta_{i-1,t}) + f(\theta_{i+1,t})) \mod 1 \qquad (1)$$

where t is the discrete time index, and i is the site index: $i = 1,\ldots L$, with L being the system size. The parameter ϵ gives the strength of the diffusive coupling between site i and its two neighbours. The local on-site map is given by

$$f(\theta) = \theta + \omega - \frac{k}{2\pi}\sin(2\pi\theta) \qquad (2)$$

where the parameter k gives the nonlinearity. This CML has been studied extensively with parallel up-dates and has a rich phase diagram with many types of attractors and strong sensitivity to initial conditions[14, 15]. In particular, this system also has regimes of spatio-temporal intermittency (STI) when evolved parallely with random initial conditions. Figs. 1 and 2 show space-time plots of the spatio-temporal intermittency observed in two different STI regimes. It is clear that no travelling wave soliton-like structures are seen in this regime. Hence, it is not necessary to introduce any asynchronicity here to destroy "solitonic" behaviour, as this system is naturally free of such spatiotemporal excitations in the parameter region studied here.

We shall now study the onset of spatiotemporal intermittency in this system. Interestingly, as mentioned before, two qualitatively distinct absorbing regions can be found in this system.

(i) When nonlinearity parameter $k = 1$, there are regions of $(\epsilon - \omega)$ space where the system goes to the synchronised spatiotemporal fixed point $\theta^\star = \frac{1}{2\pi} \sin^{-1}(\frac{2\pi\omega}{k})$. This constitutes an *unique* absorbing state (see Fig. 1). We closely scrutinise the critical behaviour at 2 critical points in this regime: $\omega = 0.064, \epsilon = 0.63775$, and $\omega = 0.068, \epsilon = 0.73277$. These mark the transition from a laminar phase to STI. The turbulent sites here are those which are different from $\theta^\star$.

(ii) When nonlinearity parameter $k = 3.1$, there are regions of $(\epsilon - \omega)$ space where sites with any value less than $1/2$ constitute the absorbing states, and sites whose values are greater than $1/2$ constitute the turbulent states (see Figs. 2 a-b). So now the absorbing states are *inifinitely many*, as also *weakly chaotic*. We study the critical behaviour at 2 critical points in this

6

regime: $\omega = 0.18, \epsilon = 0.701$, and $\omega = 0.19, \epsilon = 0.65612$.

As mentioned earlier, we initiate the evolution with random initial conditions and let the system evolve under parallel updates. The DP universality class is characterised by a set of critical exponents which describe the scaling behaviour of the quantities of physical interest. The physical quantities of interest for such systems are (a) the escape time τ, which is the number of time steps elapsed before the system reaches its laminar state and (b) the order parameter, $m(\epsilon, L, t)$, which is the fraction of turbulent sites in the lattice at time t. From finite-size scaling arguments, it is expected that τ depends on L such that

$$\tau(\omega, \epsilon) = \begin{cases} log\ L & \text{laminar phase} \\ L^z & \text{critical phase} \\ exp\ L^c & \text{turbulent phase} \end{cases}$$

Here, c is a constant of order unity, and the critical point is identified as the set of parameter values at which τ shows power-law behaviour with z being the critical exponent. At ϵ_c the critical value of the parameter ϵ (other parameters being held fixed), the order parameter $m(\epsilon, L, t)$ scales as

$$m \sim (\epsilon - \epsilon_c)^\beta, \quad \epsilon \rightarrow \epsilon_c^+. \tag{3}$$

when the critical line is approached from above. Also, at the critical ϵ_c, the order parameter is expected to satisfy the scaling relation

$$m \sim (\epsilon - \epsilon_c)^\beta, \quad \epsilon \rightarrow \epsilon_c^+. \tag{4}$$

We compute the above quantities for our CML averaged over an ensemble of 10^4 initial conditions. The dependence of τ on L for different values of

ϵ is shown on a log-log plot in Fig. 3. Fig. 3 shows this dependence at the parameter values $k = 1$, $\omega = 0.068$ (i.e. at parameter values which correspond to a unique absorbing state). It is clear from the graph that an algebraic increase can be seen at the value $\epsilon_c = 0.63775$. A similar analysis was carried out for the parameter values $k = 1$, $\omega = 0.064$, where a unique absorbing state can again be seen and gave the critical value $\epsilon_c = 0.73277$. Weakly chaotic absorbing states were seen at the parameter values $k = 3.1$, $\omega = 0.18$, and $\omega = 0.19$. Here the critical values of parameters turned out to be $\epsilon_c = 0.70100$ for the first case and $\epsilon_c = 0.65612$ for the second case. The critical exponent z was estimated at these critical values for all four cases. The log-log plot of the escape time τ against the system size L is shown in Fig. 4. It is clear that the same exponent z is seen for all four cases and turns out to lie in the range $1.58 - 1.59$ which is completely consistent with the DP value for this exponent. (See Table I).

The order parameter is expected to obey the scaling relation

$$m(\epsilon_c, L, t) \approx t^{-\beta/\nu z} \tag{5}$$

for $t << \tau$. Therefore the log-log plots of m as a function of time t for various lattice sizes must fall on one line when $t << \tau$ and the power $-\beta/\nu z$ must correspond to the slope of the graph for these regimes. The order parameter is plotted as a function of t on log-log plot in Figs. 5 and 6, where the data in Fig. 5 is obtained for the parameter values $k = 1$, $\omega = 0.068$ and $\epsilon_c = 0.63775$ (the unique absorbing state case, and that in Fig. 6 is obtained for $k = 3.1$, $\omega = 0.19$ and $\epsilon_c = 0.65612$ (the case with weakly chaotic absorbing states). In both cases, the data for $L = 50, 100, 300, 500, 1000$

collapses on to one line, the slope of which gives $-\beta/\nu z = -0.16$.

The order parameter of systems which belong to the directed percolation universality class satisfies the scaling function

$$m(\epsilon_c, L, t) \sim L^{\beta/\nu} g_{ml}(t/L^z). \tag{6}$$

at the critical value $\epsilon = \epsilon_c$. We plot the order parameter for our CML at the critical values above in Figs. 7 and 8. The data with scaled variables $M = mL^{\frac{\beta}{\nu}}$ and $T = t/L^z$ fall on one curve for various lattice sizes indicating dynamical scaling (see Figs. 7 and 8, parameter values are as given in the figure captions). This further substantiates the claim that the behaviour of the sine circle map CML falls in the directed percolation universality class.

The exponent ν can be extracted independently, by using the scaling relation

$$\tau(L, \delta) \approx \phi^z f(L/\phi), \tag{7}$$

where ϕ is the correlation length which diverges as $\phi \approx \delta^{-\nu}$ and δ is given by $\epsilon - \epsilon_c$ [16]. Therefore, ν can be obtained by adjusting it's value till the scaled variables $L\delta^\nu$ and $\tau\delta^{\nu z}$ collapse onto a single curve. Thus, the exponent β can be obtained from equation 6.

To extract further critical exponents, we obtain the correlations from the pair correlation function given by:

$$C_j(t) = \frac{1}{L} \sum_{i=1}^{L} < u_i(t)u_{i+j} > - < u_i(t) >^2 \tag{8}$$

where the brackets denote the averaging over different initial conditions. At

9

criticality one expects an algebraic decay of correlation, i.e.

$$C_j(t) \approx j^{1-\eta'}$$

where η' is the associated critical exponent. The log-log plot of the spatial correlation function at $k = 1$, $\omega = 0.064$, $\epsilon_c = 0.73277$ can be seen in Fig. 9. The log-log plot of the correlation function approaches a straight line with slope $1 - \eta'$ at large times. The value of the exponent η turns out to be 0.302, which is consistent with the directed percolation value. The values of the exponent at the other critical set of parameter values are listed in Table I. Directed percolation like behaviour is observed for the entire set.

Thus we have obtained the *complete set of static (bulk) exponents*, namely z, β, ν, η', that characterize the DP class (see Table I). Clearly the values of the exponents obtained for the coupled circle map lattice are in excellent agreement with the DP values for both unique as well as the weakly chaotic absorbing states.

The exponents also satisfy the hyperscaling relation, $2\beta/\nu = d - 2 + \eta'$, where $d = 1$.

3 Spreading Exponents

In the previous section we obtained the static exponents, also known as the bulk exponents for our CML, and found that they were in good agreement with those of DP. We shall now compute a set of dynamical exponents, called the spreading exponents, from the temporal evolution of a nearly absorbing system with a localized disturbance i.e. with only few contiguous active

k	ω	ϵ	z	β	ν	η'
1	0.068	0.63775	1.580	0.28	1.10	1.49
1	0.064	0.73277	1.591	0.28	1.10	1.50
3.1	0.18	0.70100	1.597	0.26	1.12	1.50
3.1	0.19	0.65612	1.591	0.28	1.10	1.49
DP			1.58	0.28	1.10	1.51

Table 1: Critical static exponents of the synchronously updated coupled circle map lattice for 4 critical points. The first two critical points correspond to transitions to an unique absorbing case, while the third and fourth points correspond to weakly chaotic absorbing states. The last row shows the corresponding exponents of directed percolation.

(turbulent) sites in an otherwise absorbing state. The quantities of interest are, the time dependence of $N(t)$, the number of active sites at time t averaged over all runs, $P(t)$, the survival probability, or the fraction of initial conditions which show a non-zero number of active sites (or a propagating disturbance) at time t and $R^2(t)$, the mean squared deviation from the origin of the turbulent activity averaged over surviving runs alone. The spreading exponents are obtained from the time dependence of these quantities which show scaling behaviour at criticality. At criticality, we have,

$$N(t) \approx t^\eta, \quad P(t) \approx t^{-\delta}, \quad R^2(t) \approx t^{z_s}.$$

Also, $\delta = \beta/\nu z$. We shall now compute these quantities for our system and compare them with those of DP.

For $k = 1$, we have already seen that the absorbing state is the synchronised spatiotemporal fixed point. However, when we start with a lattice with only a single active site and all other sites at the spatiotemporal fixed point, we see that the sytem goes to its absorbing state in about 10 time steps of evolution. Further the symmetric diffusive coupling in the CML indicates that the temporal spreading will be symmetric about the single active site, which is not desirable. Therefore, for good statistics and to counter the symmetric spreading, we need at least two contiguous active sites (see Fig. 10). So in our calculations, we have started with two or more contiguous active sites, while the background is fixed at $\theta^\star$. We find that the full set of spreading exponents obtained thus (see Figs. 12-14) agree within 3 % of the DP values (see Table II).

For $k = 3.1$ there is no unique absorbing configuration as above, and

any initial configuration with values less than 1/2 constitutes an absorbing background. We find that we can now obtain reasonable asymmetric spreading (and consequently the exponents) with just a single active seed [17], and these exponents are the same as those obtained from spreading from two or three contiguous active sites (see Fig. 11). Again the complete set of spreading exponents agree with those of DP within 3 % at all critical points (see Table II and Figs. 12-14).

4   Conclusions

The evaluation of the complete set of static and spreading exponents at the onset of spatiotemporal intermittency in coupled circle map lattices, shows that this transition clearly falls in the universality class of directed percolation. All the critical characteristics of directed percolation, such as hyperscaling, are fulfilled, leading to independent controls and consistency checks of the values of all the critical exponents. DP exponents are seen at low values of nonlinearity for a unique absorbing state and at high values of nonlinearity for weakly chaotic absorbing states. It is not necessary to introduce asynchronicity or an extra dimension to tune out solitonic behaviour since no solitonic behaviour is seen in this model. Thus this model constitutes a very clean system where DP exponents are very naturally seen. Model studies such as these, showing the clean correspondence between the onset of STI and directed percolation, could then lead to promising new candidates for observing DP in real phenomena.

k	ω	ϵ	η	δ	z_s
1	0.068	0.63775	0.292	0.153	1.243
1	0.064	0.73277	0.302	0.158	1.259
3.1	0.18	0.70100	0.310	0.157	1.272
3.1	0.19	0.65612	0.308	0.156	1.251
DP			0.313	0.159	1.26

Table 2: Spreading exponents of the synchronously updated coupled circle map lattice for 4 critical points. Two active seeds in an absorbing configuration is used as initial condition. For the first 2 critical points there exists an unique absorbing state, while for the third and fourth points one can have many different absorbing states and consequently many different initial absorbing backgrounds. However we notice that the exponents obtained are quite the same for different initial preparations and thus appears universal for 2 active seeds. The last row shows the corresponding exponents of directed percolation.

References

[1] K. Kaneko, ed. *Theory and Applications of Coupled Map Lattices*, (Wiley, 1993) and references therein.

[2] This type of STI is known as the type I STI in literature.

[3] Y. Pomeau, *Physica D* **23** (1986) 3.

[4] P. Grassberger, *Z. Phys. B* **47** (1982) 365; H. Hinrichsen, arXiv: cond-mat/0001070, and references therein.

[5] I. Jensen, *J. Phys. A* **29**, 7013 (1996); I. Jensen and R. Dickman, *Phys. Rev E* **48**, 1710 (1993); J.F.F. Mendes *et al*, *J. Phys. A* **27**, 3019 (1994); M.A. Munoz *et al*, *J. Stat. Phys.* **91**, 541 (1998); M.A. Munoz *et al*, *Phys. Rev E* **56**, 5101 (1997); P. Grassberger *et al*, *Phys. Rev E* **55**, 2488 (1997);

[6] H. Chate and P. Manneville,*Physica D* **32** (1998) 409.

[7] J. Rolf, T. Bohr and M.H. Jensen, *Phys. Rev. E* **57** (1998) R2503.

[8] T. Bohr *et al*, *Phys. Rev. Lett.*, **86**, 5482 (2001).

[9] S. Ciliberto and P. Bigazzi, *Phys. Rev. Lett.* **60** (1988) 286; F. Daviaud, M. Dubois and P. Berge, *Europhys. Lett.* **9** (1989) 441.

[10] M. Rabaud, S. Michalland and Y. Couder, *Phys. Rev. Lett.* **64** (1990) 184; S. Michalland and M. Rabaud, *Physica* **D 61** (1992) 197.

[11] P. Rupp, R. Richter and I. Rehberg, arXiv: cond-mat/0201308.

[12] N. Chatterjee and N. Gupte, Phys. Rev. E, **53**, 4457 (1996).

[13] P. Bak *et al*, *Solid State Comm.*, **51**, 231 (1984); K. Wiesenfeld and P. Hadley, *Phys Rev. Lett.*, **63**, 1335 (1989).

[14] G.R. Pradhan, N. Chatterjee and N. Gupte, Phys. Rev. E **65**, 046227 (2002).

[15] G.R. Pradhan and N. Gupte, *Int. J. Bifurcations and Chaos*, **11**, 2501, (2001).

[16] Jens M. Houlrik and Mogens H. Jensen, *Phys. Lett. A* **163**, 275 (1992).

[17] If we start with the very special initial background of all sites at some fixed θ_{bg}, a single active seed will of course spread symmetrically. The exponents obtained from this symmetric spreading is non-universal and varies with θ_{bg}. For instance if $\theta_{bg} = 0.4$ the spreading exponent $\eta = 0.07$, while if $\theta_{bg} = 0.0$ the $\eta = 0.05$. However, introducing a very small spread around θ_{bg} restores the DP universality.
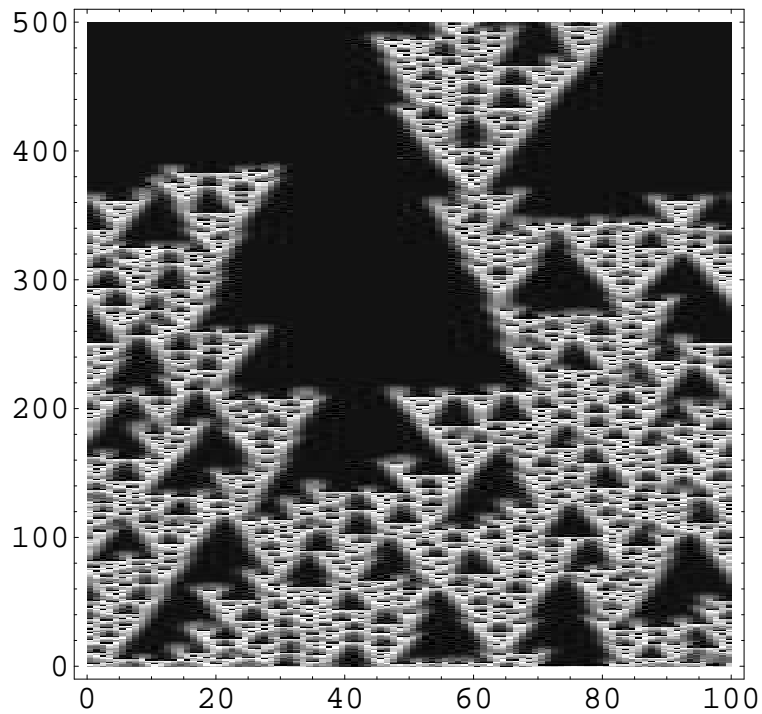
Figure 1: STI in a synchronously updated coupled circle map lattice of size $L = 100$ with parameters $k = 1$, $\omega = 0.068$, $\epsilon_c = 0.73277$. The horizontal axis is the site index $i = 1, \ldots L$ and the vertical axis is discrete time t. The absorbing region (black) has sites at the spatiotemporal fixed point of the system.
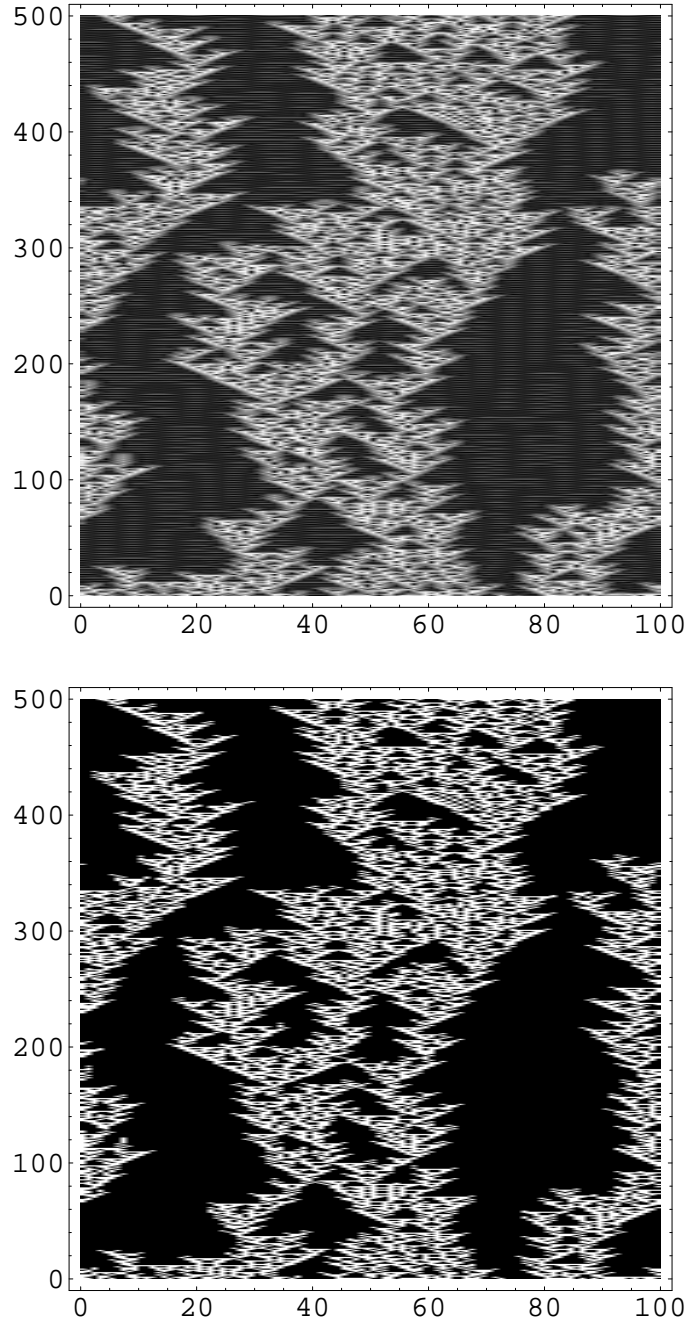
Figure 2: STI in a synchronously updated coupled circle map lattice of size $L = 100$ with parameters $k = 3.1$, $\omega = 0.18$, $\epsilon_c = 0.701$, where the absorbing region has sites below $1/2$ and is not unique. The horizontal axis is the site index $i = 1, \ldots L$ and the vertical axis is discrete time t. The top figure is obtained from a density plot of the actual θ values (the absorbing regions
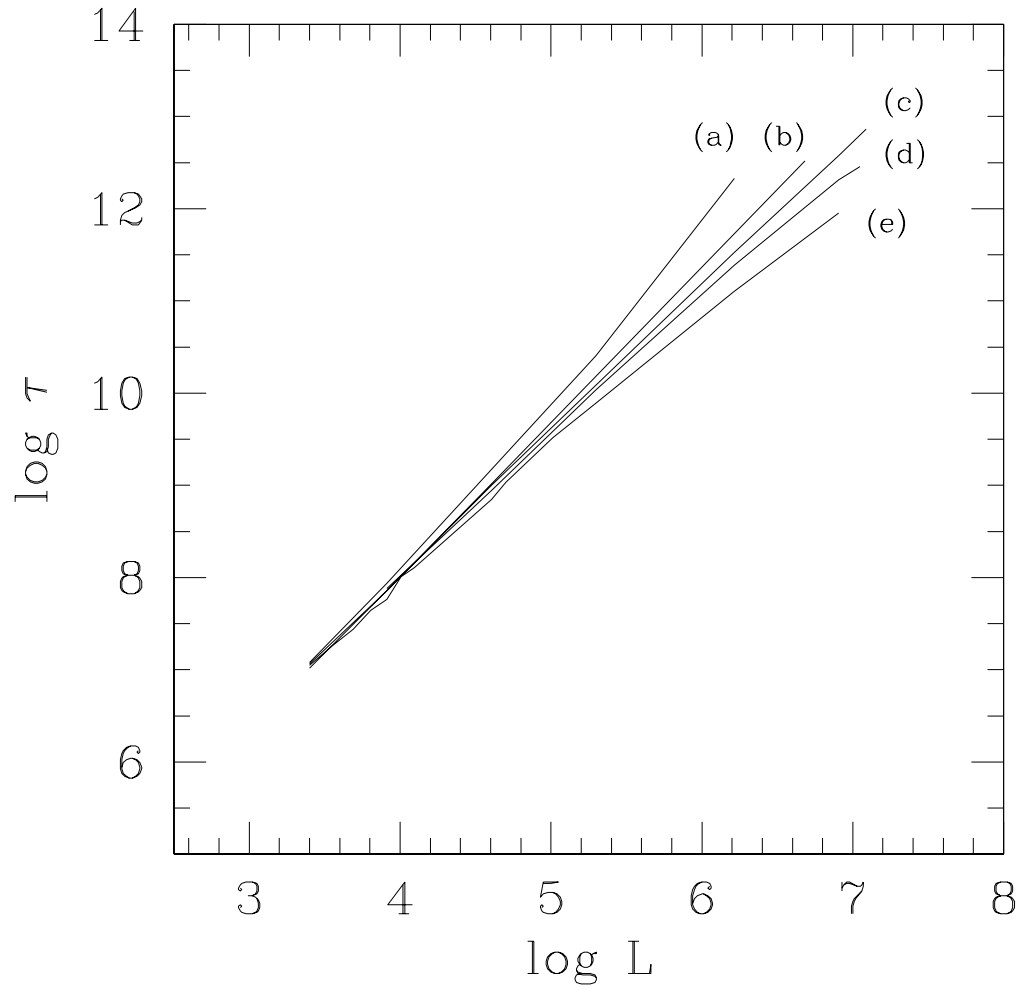
Figure 3: Log-log plot (base e) of escape time τ versus lattice size L for parameters $k = 1$, $\omega = 0.068$ and (a) $\epsilon = 0.639$, (b)$\epsilon = 0.638$, (c) $\epsilon_c = 0.63775$, (d) $\epsilon = 0.637$ and (e) $\epsilon = 0.635$.
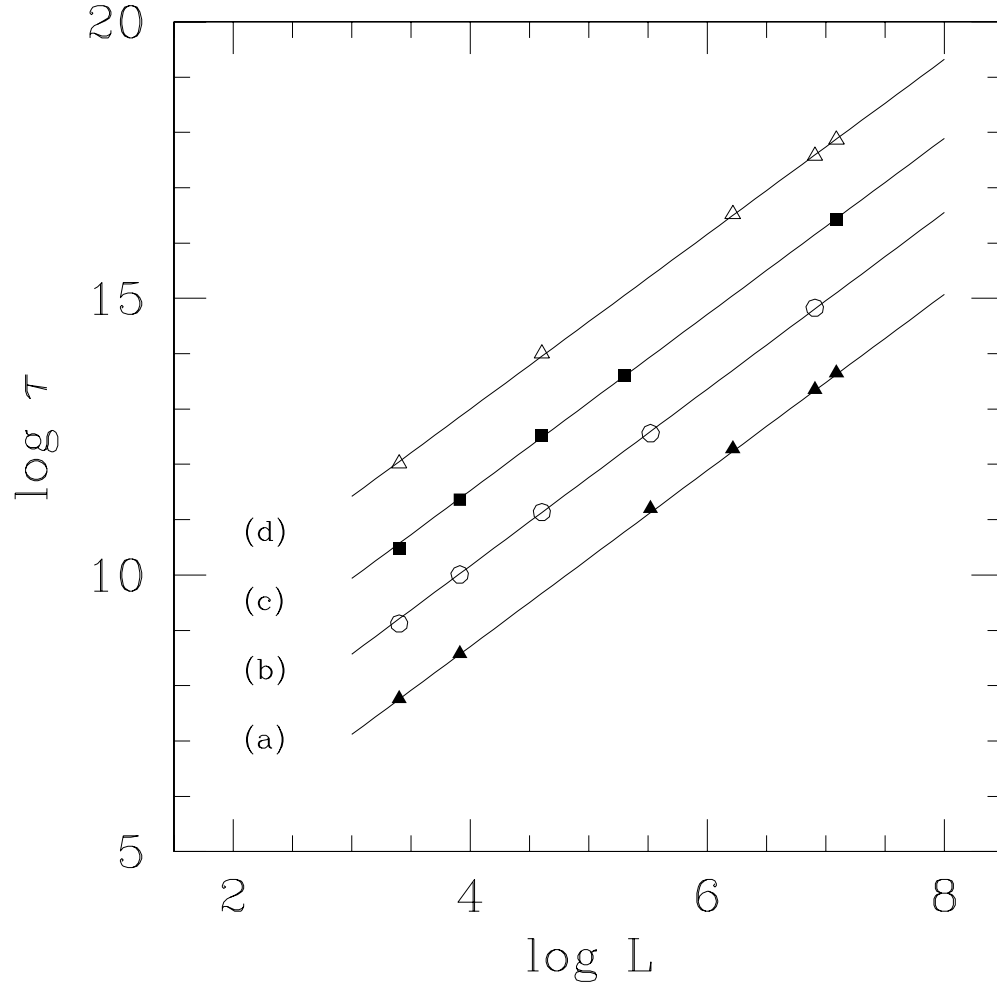
Figure 4: Log-log plot (base e) of escape time τ versus lattice size L for all 4 critical points: (a) $k = 1$, $\omega = 0.068$, $\epsilon_c = 0.63775$ and (b) $k = 1$, $\omega = 0.064$, $\epsilon_c = 0.73277$ (when there exists an unique absorbing state); (c) $k = 3.1$, $\omega = 0.18$, $\epsilon_c = 0.70100$ and (d) $k = 3.1$, $\omega = 0.19$, $\epsilon_c = 0.65612$ (with fluctuating absorbing states). Table I gives the exponent z of the power law fits for the different critical points.
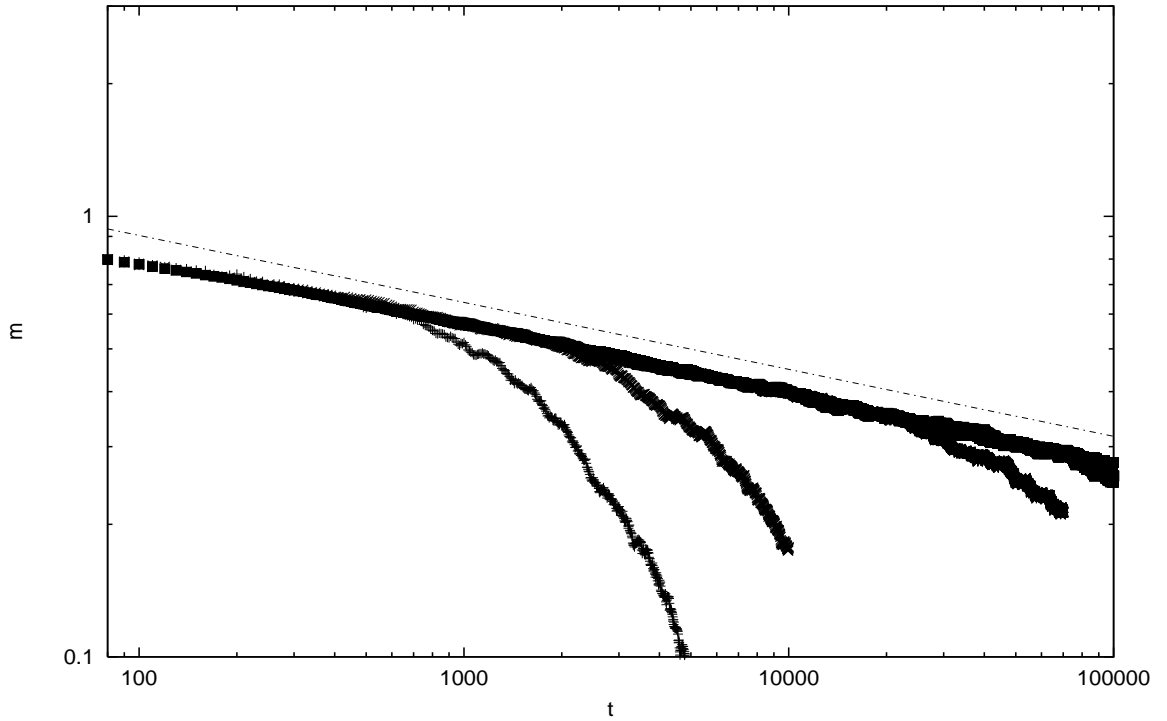
Figure 5: Log-log plot of order parameter $m(t)$ versus t for different lattice sizes at the critical point: $k = 1$, $\omega = 0.068$ and $\epsilon_c = 0.63775$ (when there exists an unique absorbing state). For $t << \tau$, the data collapses for $L = 50, 100, 300, 500, 1000$ on to one line, the slope of which gives $-\beta/\nu z = -0.16$
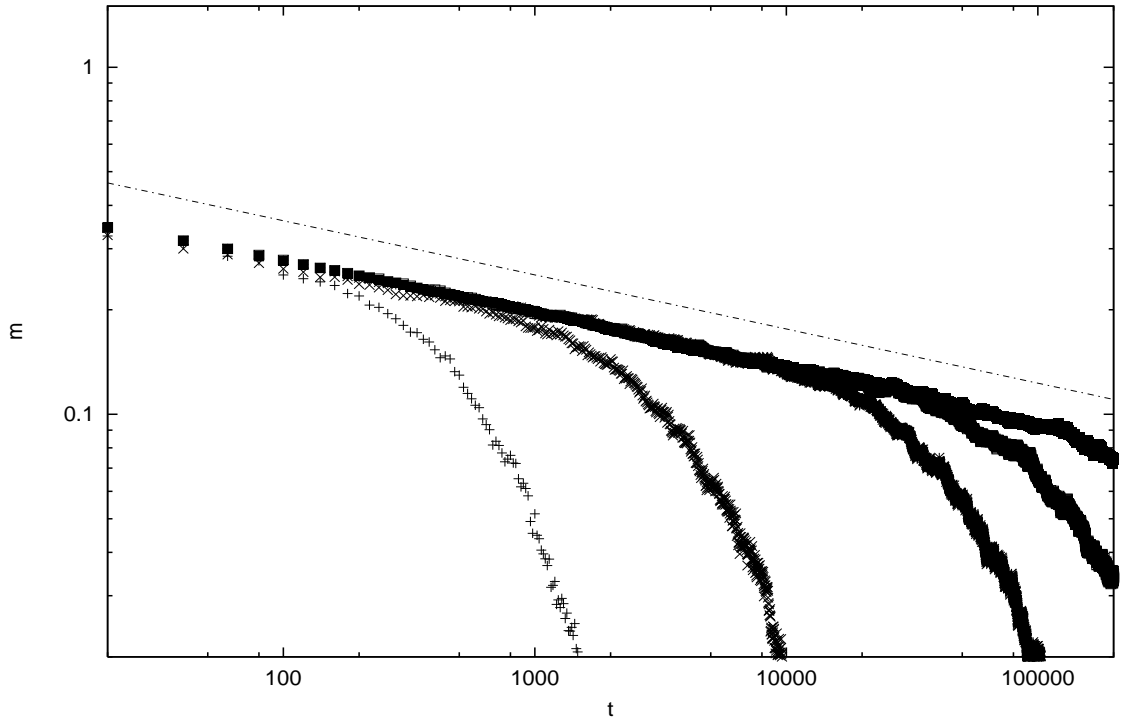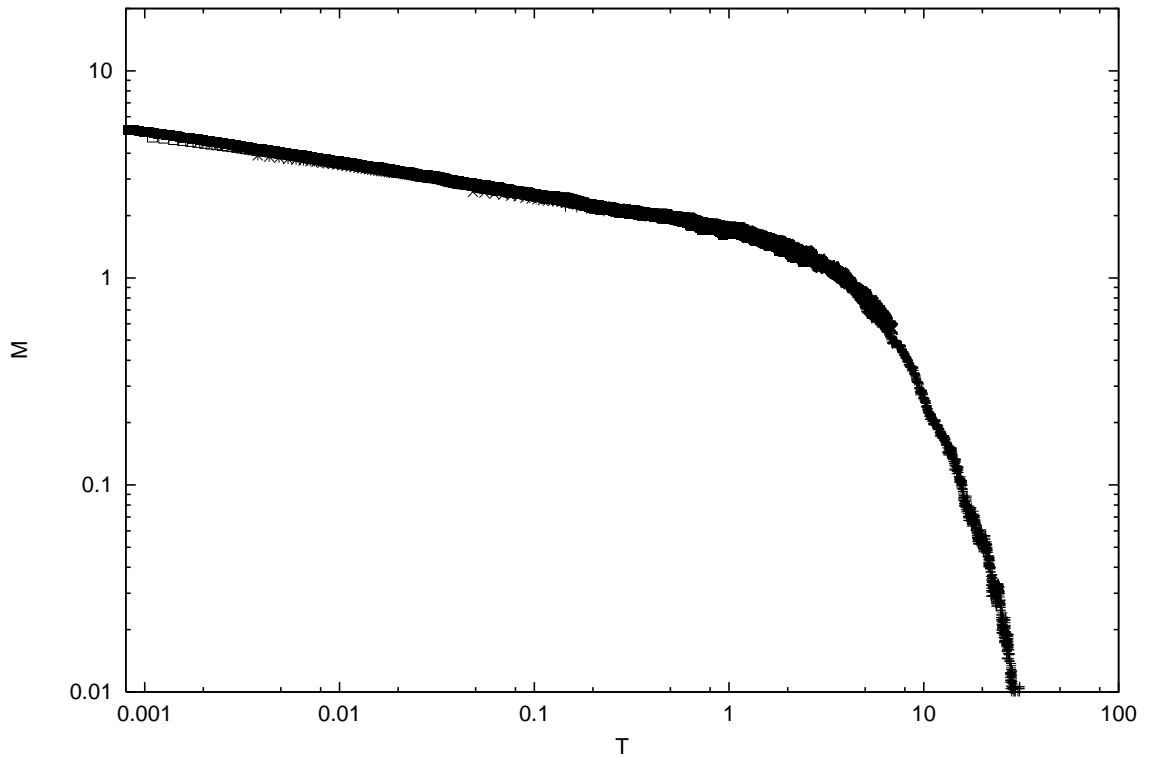
Figure 6: Log-log plot of order parameter $m(t)$ versus t for different lattice sizes at the critical point: $k = 3.1$, $\omega = 0.19$ and $\epsilon_c = 0.65612$ (a case with inifinitely many absorbing states). For $t << \tau$, the data collapses for $L = 50, 100, 300, 500, 1000$ on to one line, the slope of which gives $-\beta/\nu z = -0.16$.
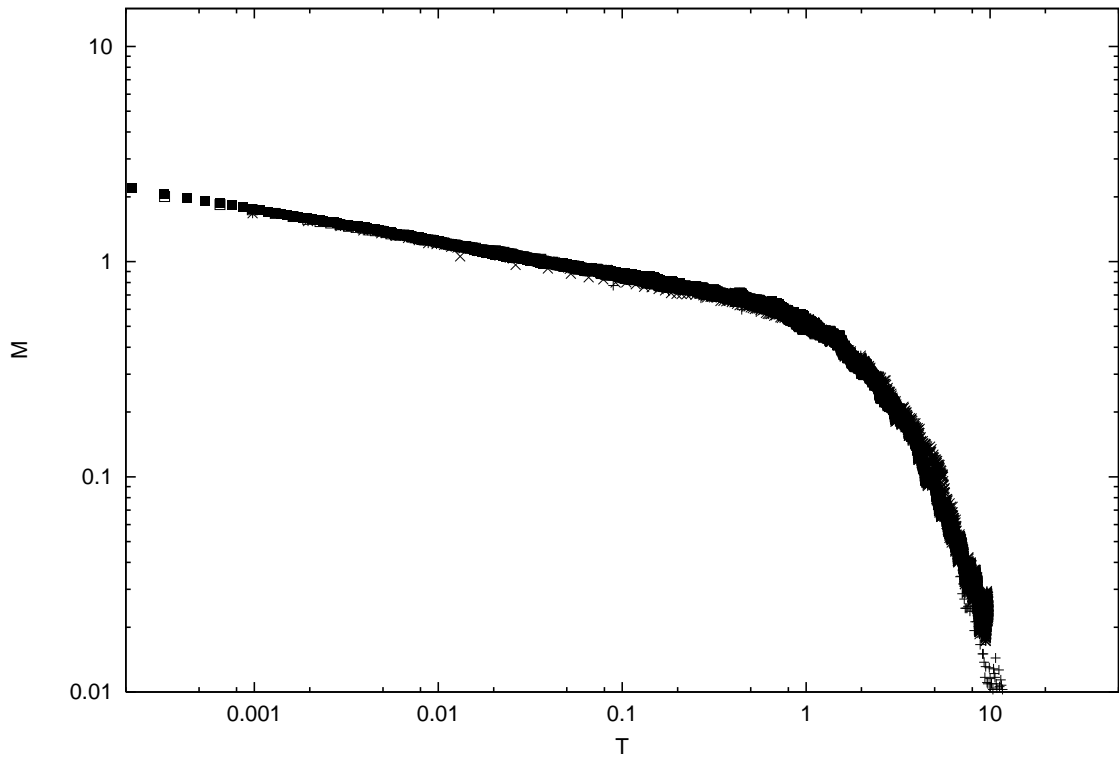
Figure 7: Log-log plot of $M = mL^{\beta/\nu}$ vs $T = t/L^Z$ at the critical point: $k = 1$, $\omega = 0.068$ and $\epsilon_c = 0.63775$ (when there exists an unique absorbing state). This rescaling of the order parameter according to Eqn. 6 yields independent estimates for β/ν and z. The data for system sizes L ranging from 2^4 to 2^{10} collapses onto one curve.
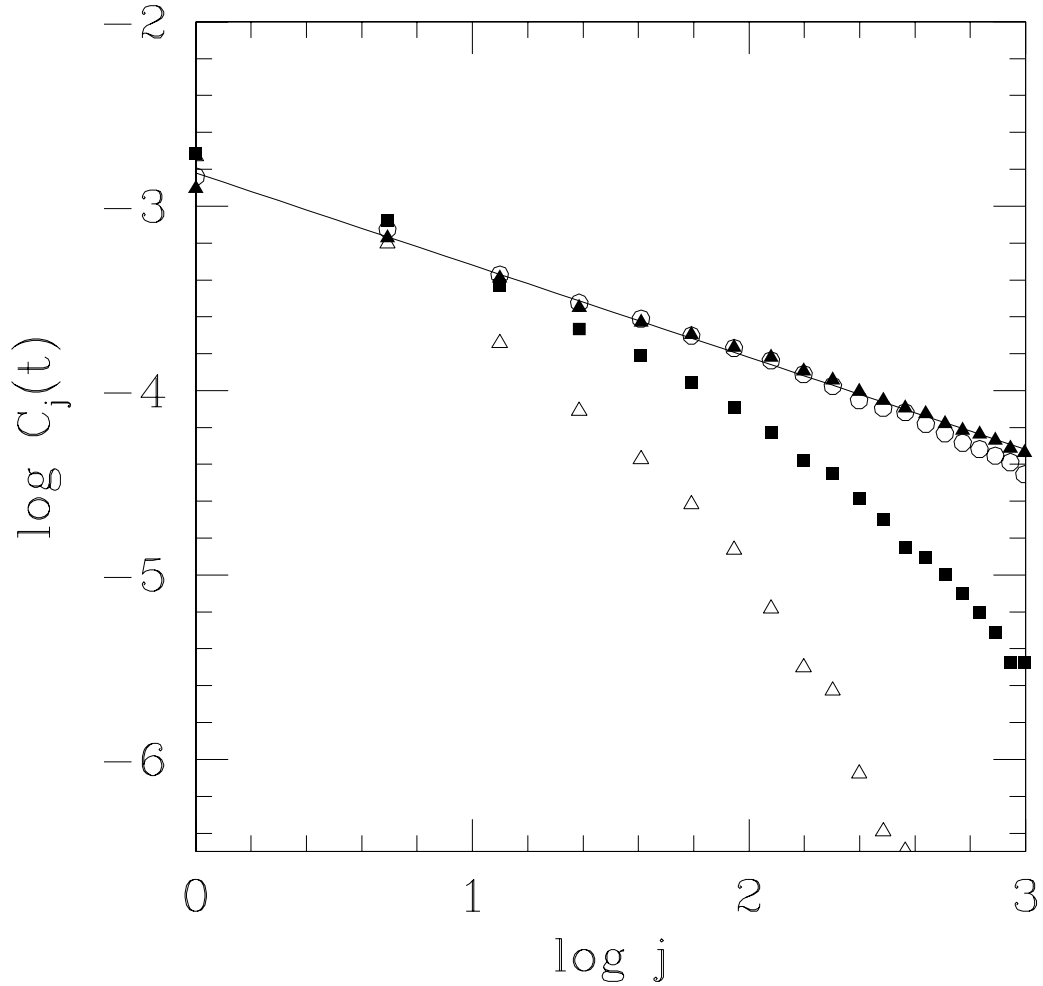
Figure 8: Log-log plot of $M = mL^{\beta/\nu}$ vs $T = t/L^Z$ at the critical point: $k = 3.1$, $\omega = 0.19$ and $\epsilon_c = 0.65612$ (when there are weakly chaotic absorbing states). This rescaling of the order parameter according to Eqn. 6 yields independent estimates for β/ν and z. The data for system sizes L ranging from 2^4 to 2^{10} collapses onto one curve.

Figure 9: Log-log plot (base e) of the spatial correlation function $C_j(t)$ vs j at various times t ($= 100, 300, 500, 1000$) at the critical point: $k = 1$, $\omega = 0.064$, $\epsilon_c = 0.73277$. $C_j(t)$ approaches a straight line with slope $1 - \eta'$ for large times indicating an algebraic decay.
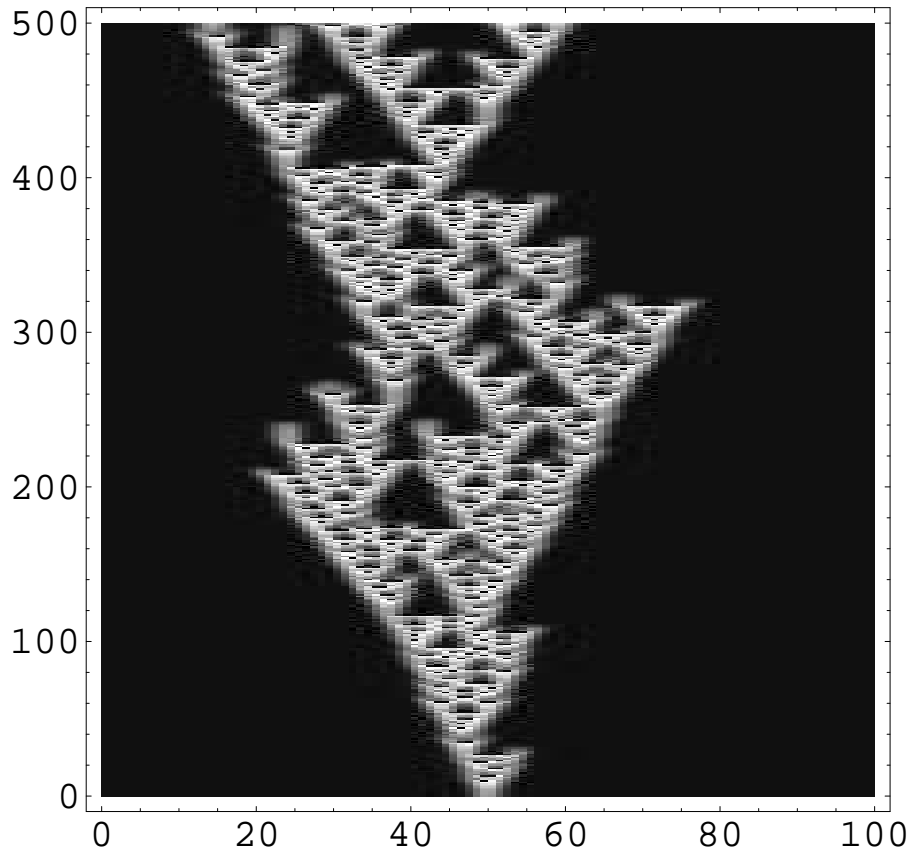
Figure 10: Spreading of 2 active seeds in an otherwise absorbing lattice of size $L = 100$ at critical point $k = 1$, $\omega = 0.068$, $\epsilon_c = 0.73277$. The horizontal axis is the site index $i = 1, \ldots L$ and the vertical axis is discrete time t. The absorbing region (black) is unique here, with all sites at the spatiotemporal fixed point of the system.
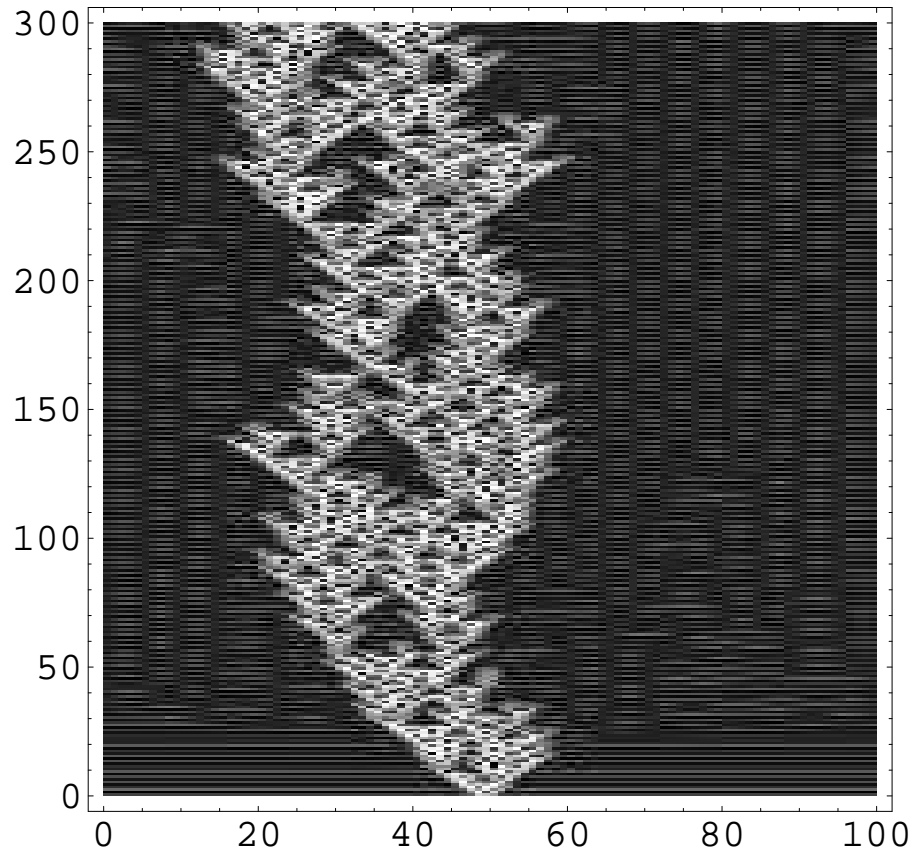
Figure 11: Spreading of 2 active seeds in an otherwise absorbing lattice of size $L = 100$ at critical point $k = 3.1$, $\omega = 0.18$, $\epsilon_c = 0.701$. The horizontal axis is the site index $i = 1, \ldots L$ and the vertical axis is discrete time t. The absorbing region (dark) has all sites below $1/2$ and is not unique.
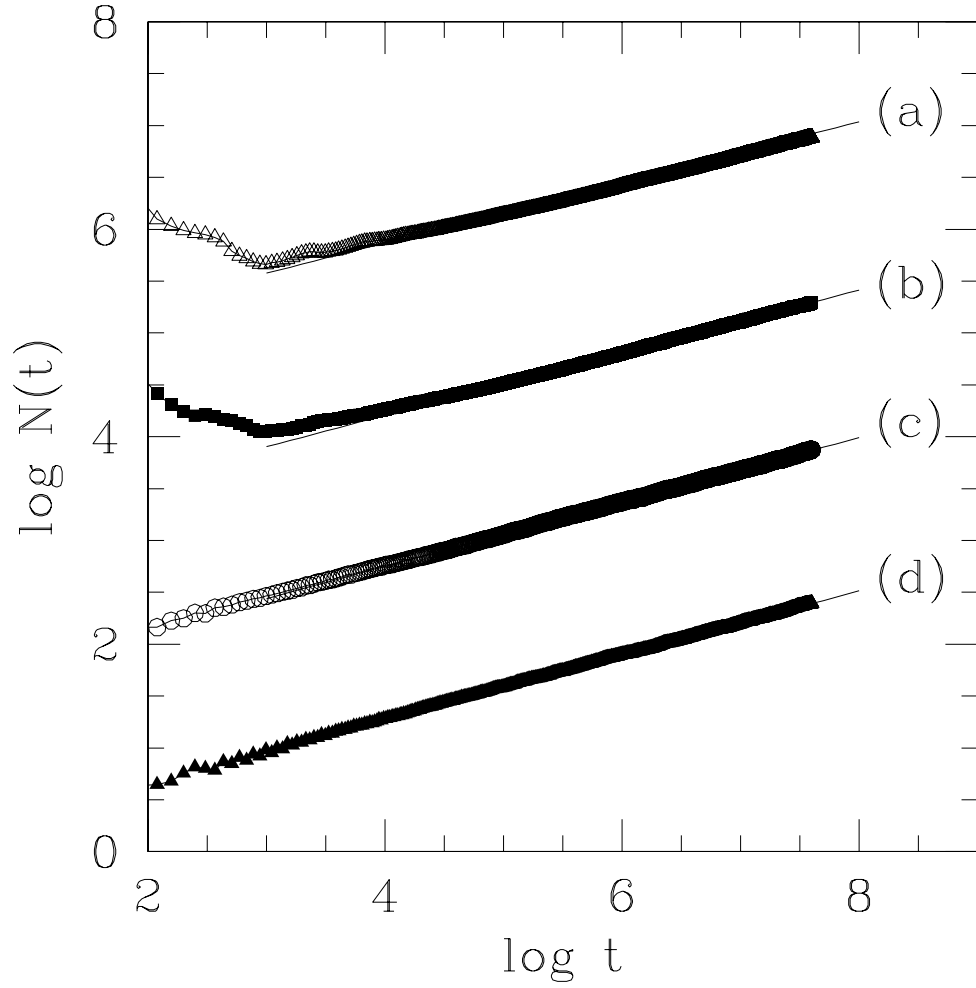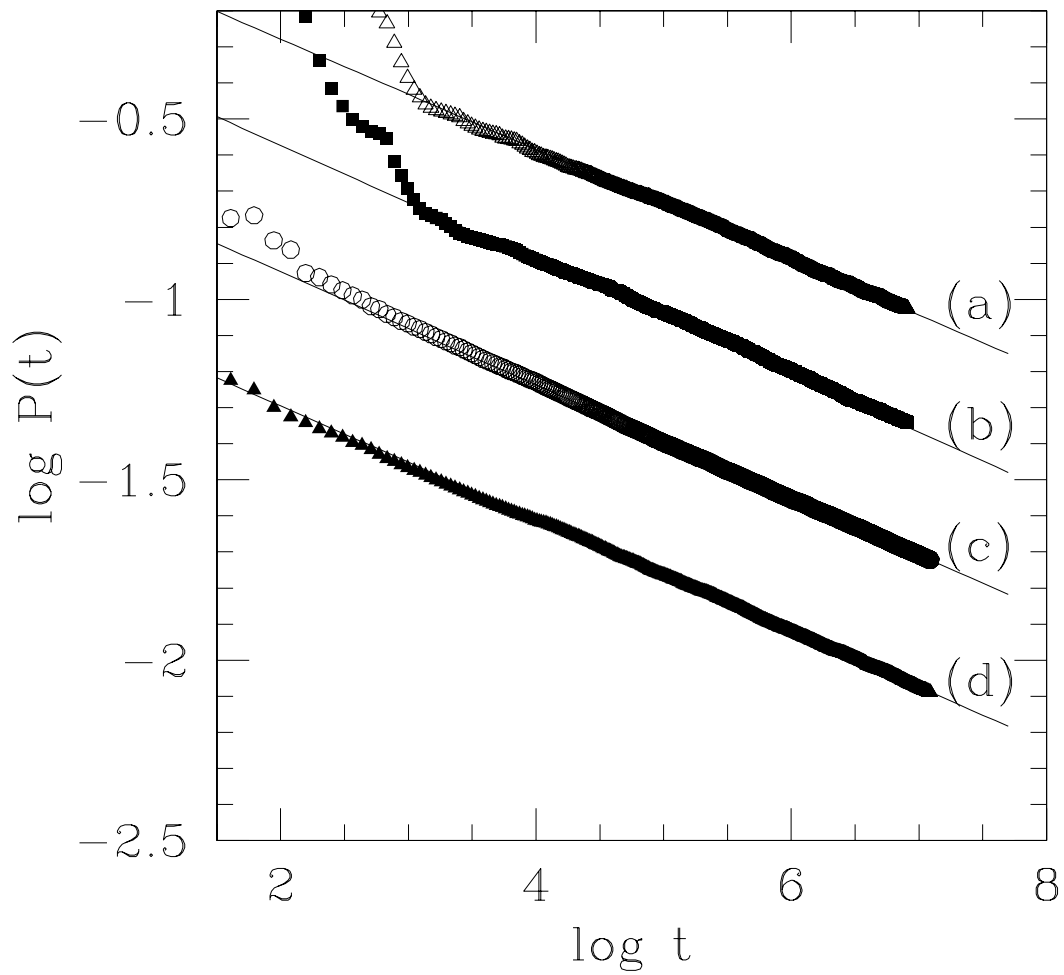
Figure 12: Log-log plot (base e) of $N(t)$ vs t for all 4 critical points: (a) $k = 1$, $\omega = 0.068$, $\epsilon_c = 0.63775$; (b) $k = 1$, $\omega = 0.064$, $\epsilon_c = 0.73277$; (c) $k = 3.1$, $\omega = 0.18$, $\epsilon_c = 0.70100$ and (d) $k = 3.1$, $\omega = 0.19$, $\epsilon_c = 0.65612$. Table II gives the exponent η of the power law fits for the different critical points.

Figure 13: Log-log plot (base e) of of $P(t)$ vs t for all 4 critical points: (a) $k = 1$, $\omega = 0.068$, $\epsilon_c = 0.63775$; (b) $k = 1$, $\omega = 0.064$, $\epsilon_c = 0.73277$; (c) $k = 3.1$, $\omega = 0.18$, $\epsilon_c = 0.70100$ and (d) $k = 3.1$, $\omega = 0.19$, $\epsilon_c = 0.65612$. Table II gives the exponent δ of the power law fits for the different critical points.
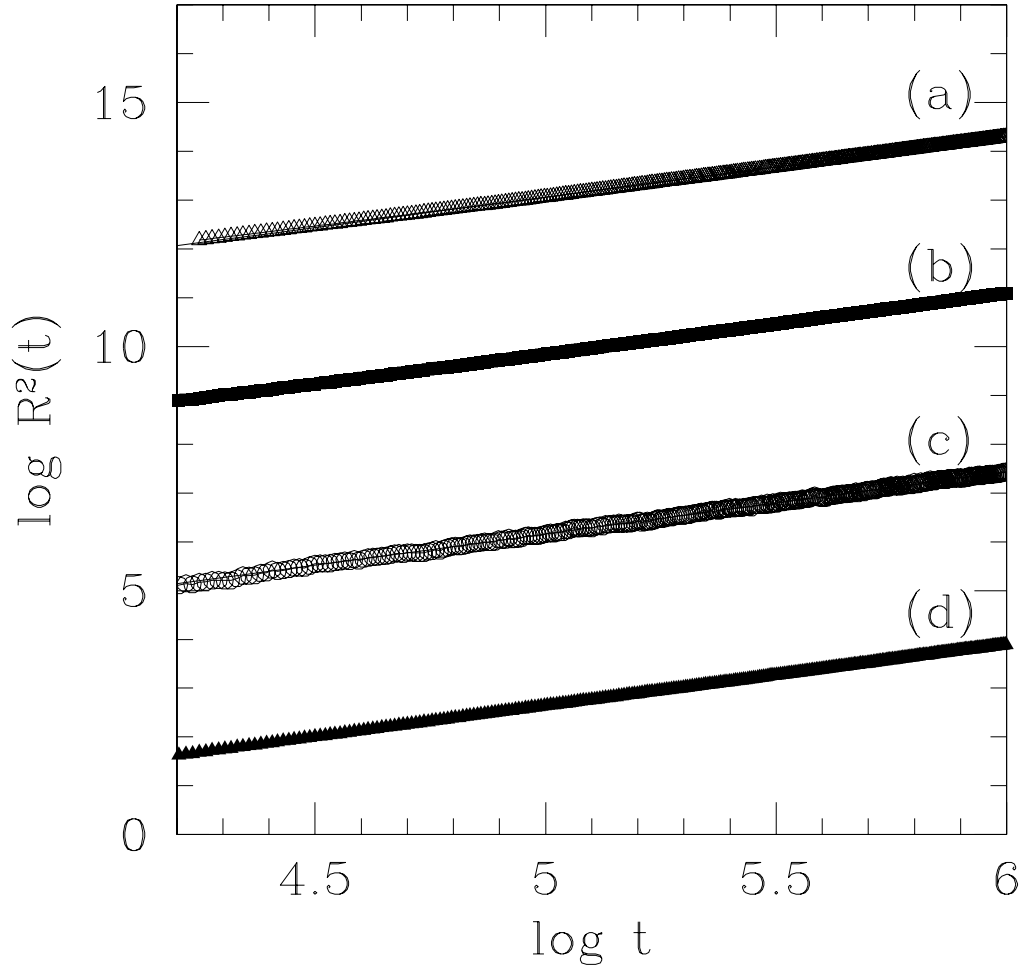
Figure 14: Log-log plot (base e) of $R^2(t)$ vs t for all 4 critical points: (a) $k = 1$, $\omega = 0.068$, $\epsilon_c = 0.63775$; (b) $k = 1$, $\omega = 0.064$, $\epsilon_c = 0.73277$; (c) $k = 3.1$, $\omega = 0.18$, $\epsilon_c = 0.70100$ and (d) $k = 3.1$, $\omega = 0.19$, $\epsilon_c = 0.65612$. Table II gives the exponent z_s of the power law fits for the different critical points.